

## Disorder and localization at the LaAlO<sub>3</sub>/SrTiO<sub>3</sub> heterointerface

Franklin J. Wong,<sup>1,2</sup> Rajesh V. Chopdekar,<sup>1</sup> and Yuri Suzuki<sup>1,2</sup><sup>1</sup>*Department of Materials Science and Engineering, University of California, Berkeley, California 94720, USA*<sup>2</sup>*Materials Sciences Division, Lawrence Berkeley National Laboratory, Berkeley, California 94720, USA*

(Received 18 July 2010; revised manuscript received 3 September 2010; published 6 October 2010)

Through low-temperature electrical transport and magnetotransport, we investigate the role of disorder on the metallicity at the (001) LaAlO<sub>3</sub>/SrTiO<sub>3</sub> heterointerface. We observe a trend of reduced mobility in higher sheet carrier concentration samples, and therefore speculate that disorder and carriers are introduced concomitantly in purely polar instability-induced metallic interfaces. Magnetotransport distinctly reveals stronger spin-orbit interaction in higher carrier concentration samples. The competition between spin-orbit scattering and inelastic scattering is explored through a temperature dependence study of the magnetotransport.

DOI: 10.1103/PhysRevB.82.165413

PACS number(s): 73.50.Jt, 73.20.Fz, 72.80.Ga, 75.70.Tj

The discovery of quasi-two-dimensional (2D) metallicity in (001) LaAlO<sub>3</sub>/SrTiO<sub>3</sub> (LAO/STO) heterostructures<sup>1</sup> has generated significant amount of research to understand the origin of the metallicity. It is now generally agreed upon that, under appropriate deposition conditions, the metallicity is due to carrier redistribution at the interface and not oxygen defects in the STO substrates.<sup>2–5</sup> A superconducting state has been demonstrated by some,<sup>6–13</sup> whereas long-range magnetism<sup>3,11</sup> and magnetic inhomogeneities<sup>14</sup> have been suggested by others. As low-dimensional materials are more susceptible to localization effects at low temperatures arising from disorder,<sup>15</sup> the presence and role of disorder must be taken into account when discussing the ground state of the heterointerface. The range of behaviors in ostensibly identical LAO thin films grown on single crystal STO substrates by different groups<sup>6–14</sup> is an indication that the heterointerface may be subject to the effects of other kinds of disorder besides oxygen vacancies.

Previous magnetotransport studies showed in-plane magnetoresistance (MR) values ranging from a few percent (both positive and negative)<sup>9,13</sup> to as large as  $-60\%$  (Ref. 11) in a field of a few teslas. Given the variation in these results alone, there is a need to identify possible origins and effects of disorder to relate findings from different studies. In electrostatically gated LAO/STO samples, interfacial electronic properties can be modified presumably independent of disorder. A number of groups have fabricated field-effect devices of LAO/STO, modulating the electric field at the interface to explore interfacial insulator-metal transition,<sup>16</sup> superconductivity,<sup>9,10,12,13</sup> and Rashba spin-orbit interaction.<sup>12,13</sup> The tunability of superconducting transitions have been attributed to changes in carrier concentration<sup>7,13</sup> as well as mobility.<sup>10</sup> Moreover, independent of electrostatic doping, the thickness of the LAO film has also been suggested to be an important parameter that affects carrier transport.<sup>17</sup> However, a detailed study of the relationship and competition between disorder and carrier concentration is still lacking.

In this paper, we report the relationship between the degree of disorder and sheet carrier concentration at metallic LAO/STO interfaces arising from polar interface instability. From low-temperature Hall effect measurements, we find that the introduction of carriers is accompanied by an increase in static scattering centers near the interface. Magne-

totransport measurements at low temperatures with the magnetic field parallel to the interface on a series of LAO films grown on STO substrates reveal a competition between weak localization and antilocalization effects. Spin-orbit interaction appears to be greater in samples with higher sheet carrier concentration. Enhanced spin-orbit coupling and the anisotropy between in-plane and out-of-plane magnetotransport are properties unique to the 2D metallic channel, not readily attainable in bulk electron-doped STO.

LAO films of thicknesses ranging from 1.6 to 14 nm were deposited on TiO<sub>2</sub>-terminated single crystal (001) STO substrates at 700 °C and in  $2.5 \times 10^{-5}$  Torr of oxygen by pulsed laser deposition. A KrF laser was pulsed at an energy density of approximately 1.4 J/cm<sup>2</sup> at 2 Hz. A combination of x-ray reflectometry and Rutherford backscattering spectrometry was used to measure film thicknesses. All of the electrical transport measurements were performed in the van der Pauw geometry with the applied field perpendicular (out of plane) and parallel (in plane) to the interface. For in-plane magnetotransport measurements, the field was applied at 45° to the sample edge directions of [100] and [010].

We use LAO film thickness as a means to achieve samples with varying sheet carrier concentration values. Figure 1(a) shows the sheet carrier concentration at 275 K as a function of thickness. The thinner films generally have lower sheet carrier (electronlike) concentration for LAO film thickness values up to 5 nm, above which the sheet carrier concentration appears to saturate.

Electrical transport data at 3 K show a general trend of

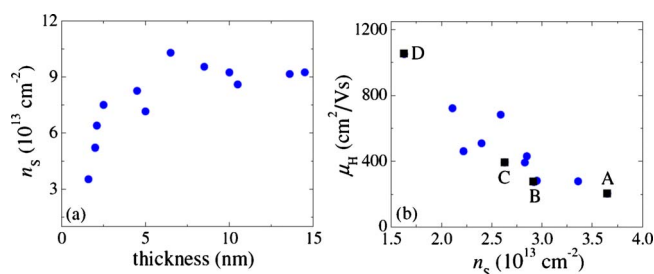


FIG. 1. (Color online) (a) Sheet carrier concentration ( $n_s$ ) at 275 K of heterointerfaces of different LAO film thickness. (b) Mobility ( $\mu_H$ ) versus sheet carrier concentration at 3 K of the different samples.

TABLE I. Summary of sheet carrier concentration ( $n_S$ ), Hall mobility ( $\mu_H$ ), and estimated mean free path ( $\lambda$ ) at 3 K, as well as LAO film thickness ( $t$ ) of samples A–D.

Sample	$n_S$ ( $\text{cm}^{-2}$ )	$\mu_H$ ( $\text{cm}^2/\text{V s}$ )	$\lambda$ (nm)	$t$ (nm)
A	$3.65 \times 10^{13}$	203	20.3	11
B	$2.92 \times 10^{13}$	273	24.4	13.5
C	$2.63 \times 10^{13}$	393	33.3	5
D	$1.63 \times 10^{13}$	1052	70.2	4

decreasing electron mobility with increasing interfacial sheet carrier concentration [Fig. 1(b)]. At low temperatures where inelastic scattering is minimized, the mobility is a measure of the degree of disorder associated with static elastic scattering sites for carriers. Our mobility values are comparable to those observed by other groups.<sup>6,10,11,18,19</sup> These values are considerably less than those of bulk electron-doped STO crystals, ranging from  $\sim 1000$  to  $5000 \text{ cm}^2/\text{V s}$  for oxygen vacancy doping and  $\sim 3000$  to  $20\,000 \text{ cm}^2/\text{V s}$  for Nb doping.<sup>20</sup> The lower interfacial mobility values obtained in the LAO/STO heterointerfacial metallic channels suggest that the effects of disorder must be considered.

The increase in sheet carrier concentration coincident with a decrease in mobility, and hence an increase in disorder, suggests that the generation of carriers is associated with a greater amount of scattering centers or enhanced scattering. The carrier concentration and mobility values govern the low-temperature transport behaviors and therefore will be used herein to refer to the different samples. Specifically we focus on four samples (A–D) labeled in Fig. 1(b), and some of their parameters are listed in Table I.

Low-temperature transport data of samples A–D reveal upturns in sheet resistance that are more pronounced and occur at higher temperatures in samples with higher carrier concentration (Fig. 2). In this temperature regime, the higher carrier concentration, lower mobility samples are more resistive. Both weak localization<sup>9</sup> and Kondo scattering<sup>3</sup> have been invoked to explain the existence of such sheet resistance minima. Whereas the sheet resistance values and the magnitude of the sheet resistance upturn appear to vary substantially from sample to sample, the values for the correction to conductance,  $[R_S^{\text{min}} - R_S(T)]/R_S^{\text{min}}R_S(T)$ , of all of the

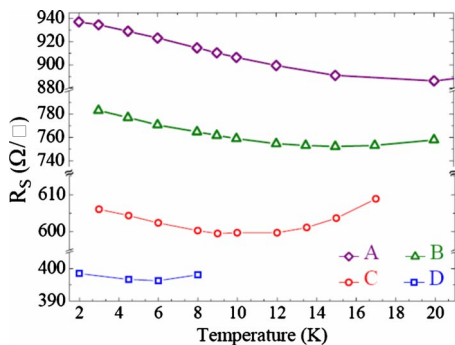


FIG. 2. (Color online) Temperature-dependent sheet resistance of samples A–D.

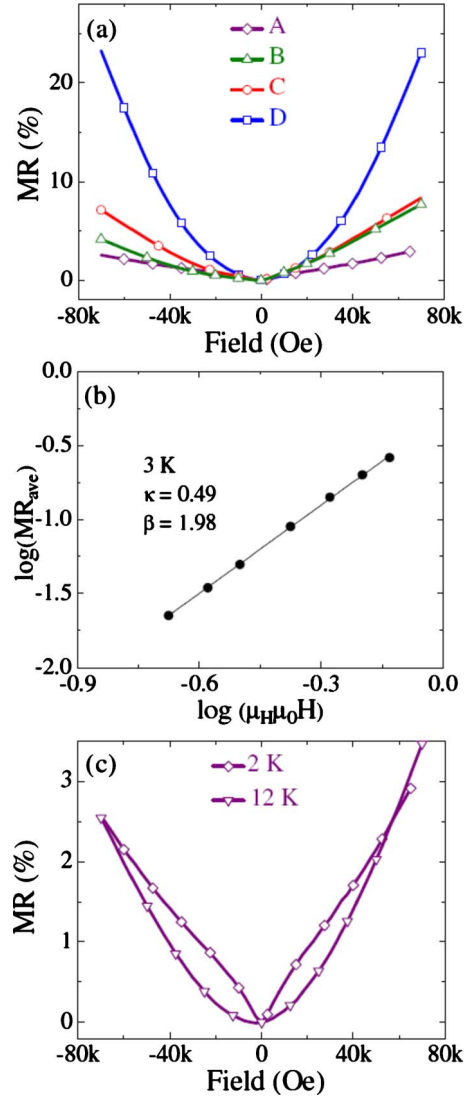


FIG. 3. (Color online) (a) Out-of-plane MR of samples A–D at 3 K. (b) Kohler plot for sample D at 3 K and the corresponding fitting parameters. (c) Out-of-plane MR of sample A at 2 and 12 K.

samples are on the order of  $-pe^2 \ln 10 / \pi h = -5.7 \times 10^{-5} \Omega^{-1}$  per decade for  $p=2$ . Although the curves of the quantum correction to conductance do not have a strict logarithmic dependence on temperature, as would be expected for weak localization, localization phenomena cannot be completely dismissed in describing the low-temperature electrical transport data. In fact, electron-electron correlation, spin-orbit interaction, and possible long-range ordering may account for the deviation from a purely logarithmic temperature dependence.

Magnetotransport measurements provide additional insight into the role of disorder and localization effects, especially important in low-dimensional systems such as the LAO/STO heterointerface. Figure 3(a) shows the MR curves at 3 K with the magnetic field applied normal to the sample plane. The positive MR is attributed to orbital effects, often called ordinary MR. We expect the ordinary MR to follow Kohler's rule:  $\text{MR} = F(H/\rho) \approx F'(\mu H)$ , where  $H$  is the magnetic field,  $\rho$  is the sample resistivity, and  $F$  and  $F'$  are

monotonic functions. Indeed, the positive MR becomes larger with increasing field and in higher mobility samples. A Kohler plot can be made using MR values that are symmetrized with respect to applied field ( $MR_{ave}(H) = 1/2[MR(H) + MR(-H)]$ ). Such is common practice, and it is valid here because the asymmetry of the MR in positive and negative fields is due to geometric, not intrinsic, effects. In addition, despite the seemingly high fields applied, we find that  $\omega_c \tau = \mu_H \mu_0 H < 1$ , indicating that we are in the low-field limit. Experimentally, the ordinary MR is commonly found to be of the form  $\kappa(\mu_H \mu_0 H)^\beta$ . To be as general as possible, we allow both  $\kappa$  and  $\beta$  to be fitting parameters. Figure 3(b) shows a fit to the MR of sample D at 3 K for data from 20 to 70 kOe for  $\kappa=0.49$  and  $\beta=1.98$ . The scaling of the out-of-plane MR to the mobility-field product leads us to believe that ordinary orbital effects are indeed dominant.

A zoomed-in view of the MR of sample A, which has the highest carrier concentration, at 2 K shows a deviation from parabolic field-dependent behavior in the form of a cusp at lower field values [Fig. 3(c)]. This cusp suggests the onset of an additional contribution to the MR that disappears at higher temperatures, and is most evident in sample A partly because it has the lowest mobility and therefore the lowest ordinary MR.

Magnetotransport with the applied field parallel to the interface enables us to separate out orbital effects from the MR. There appears to be no ordinary MR contribution [Fig. 4(a)] for all of the samples. The suppression of the ordinary MR contribution suggests that the thickness of the interfacial metallic layer is within one carrier mean free path. Using an isotropic, parabolic band approximation, we estimate the mean free path of sample A at 3 K, for example, to be 20.3 nm (Table I). Because the ordinary component to MR is suppressed, other contributions can be isolated and therefore become more discernible. Moreover, the MR anisotropy illustrates the quasi-2D nature of metallicity at the LAO/STO interface. Examining the MR curves of Fig. 4(a), we see that there are two regimes, a positively sloped MR portion in lower fields and negatively sloped in higher fields, resulting in a local MR maximum. Note that the low-field positive component is barely visible in sample D, which has the lowest carrier concentration. Figure 4(b) shows that the in-plane positive MR contribution increases with decreasing temperature and is most likely linked to the cusp observed in the out-of-plane MR of sample A at 2 K [Fig. 3(c)].

The existence of a quasi-2D electron gas suggests the presence of band bending at the LAO/STO interface that can provide for electron confinement. Possible origins include the presence of some form of interface charges and chemical bonding effects at the interface. Band bending that would result in an interfacial mobile electron channel necessitates the possible interface charges be positive. We consider specifically the possibility of trapped interface charges on the LAO side of the heterojunction and their origin. Beyond the critical thickness of the LAO film of four unit cells for an insulator-metal transition,<sup>2</sup> the LAO valence band edge becomes lower than the conduction band edge of STO, and electrons tunnel from the LAO to the STO side, where they can become mobile. Here the LAO is considered to be the source of carriers, manifested in the presence of immobile

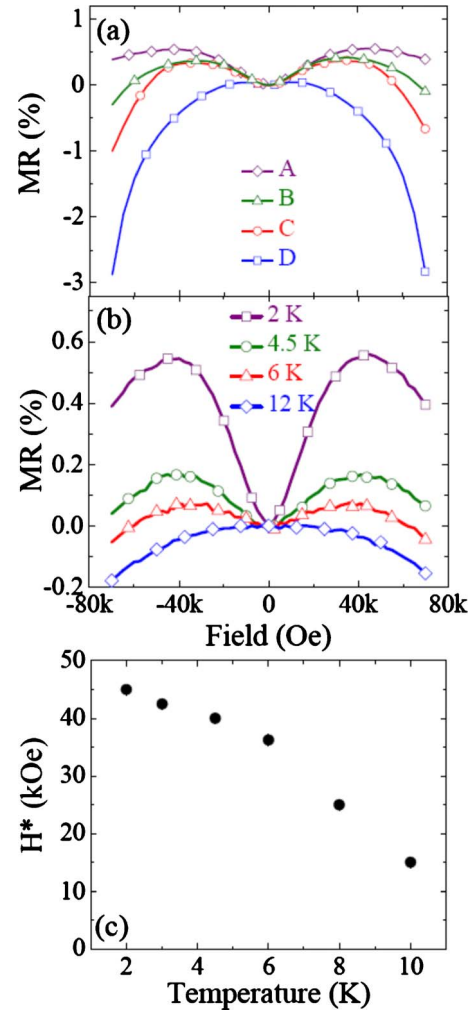


FIG. 4. (Color online) (a) In-plane MR of samples A–D at 2 K. (b) In-plane MR of sample A at various temperatures. (c) Temperature-dependent crossover field ( $H^*$ ), as defined in the text, in the in-plane MR of sample A.

holes on the LAO side. The formation of hole polarons has been considered and thought to be likely in related oxides.<sup>21</sup> Localized holes in LAO near the interface can enhance band bending at the heterojunction, thus confining the electron channel to be quasi-2D. At the same time, these holes can also act as scattering centers that limit the magnitude of carrier mobility and may be the relevant form of disorder here.

The assumption of localized holes in LAO being the source of carriers at the interface as well as elastic scattering centers accounts for the observed trend of higher carrier concentration accompanied by reduced mobility in thicker films [Fig. 1(b)]. When the film thickness becomes larger than the physical extent of band bending on the LAO side, the carrier concentration levels off with further increases in film thickness, thus explaining the saturation of carrier concentration for film thicknesses greater than about 5 nm [Fig. 1(a)]. We emphasize that other forms of interfacial charges and any interfacial bonding effects<sup>22</sup> can also directly influence interfacial band bending and can readily be incorporated into our description.

The upturn in sheet resistance and the in-plane MR curves

may be explained by weak localization effects. We speculate the negative MR observed in sample D, for example, to be attributed to weak localization, to which all 2D materials with any degree of disorder are susceptible.<sup>15</sup> The positive ordinary MR contribution for this sample [Fig. 3(a)] for the field applied out of plane conceals the negative contribution due to localization effects; this negative contribution becomes visible when the field is applied in plane [Fig. 4(a)]. As the carrier concentration increases from sample D to sample A, a positive in-plane MR component gradually emerges [Fig. 4(a)]. We will refer to the field corresponding to the positive local maximum in the in-plane MR as  $H^*$ . A crossover from positively to negatively sloped MR similar to that exhibited by sample A below 12 K has been observed in a number of 2D disordered metals with crossover fields as high as  $\sim 10$  kOe in Bi films<sup>23</sup> and greater than 25 kOe in Au films.<sup>24</sup> This feature is attributed to antilocalization effects due to increasing spin-orbit interaction<sup>25,26</sup> from sample D to A. Although STO does not contain particularly heavy elements, spin-orbit interaction can be strengthened by heterointerfacial and surface electric fields.<sup>27,28</sup> For the metallic LAO/STO heterointerface arising from polar instability, the interfacial electric field is enhanced by the accumulation of mobile electrons on the STO side and perhaps trapped holes on the LAO side, resulting in large spin-orbit coupling. Caviglia *et al.*<sup>13</sup> reported similar  $H^*$  values over a range of gate voltages at 1.5 K; since the mobility value, as deduced from the reported electron diffusivity, of their sample at zero bias is comparable to that of sample A, the spin-orbit scattering times  $\tau_{so}$  should likewise be comparable.

Quantitative extraction of  $\tau_{so}$  and the electron dephasing time  $\tau_\phi$  of samples is complicated by the lack of a precise measurement of the exact metallic channel thickness.<sup>23</sup> Regardless, the temperature dependence of MR allows for comparison of the relative rates of spin-orbit and inelastic scattering. We expect the dominant carrier dephasing mechanism to be inelastic scattering. Antilocalization effects are visible when  $\tau_{so}$  is less than the inelastic scattering time  $\tau_{in}$ , and therefore disappear at higher temperatures, as in Fig.

4(b). For sample A, this crossover occurs at about  $12 \pm 2$  K, below which the spin-orbit scattering rate is higher. To clearly show this progression of MR, we plot  $H^*$  with respect to temperature in Fig. 4(c).

The interdependent generation of carriers on the STO side and disorder near the interface appears to be a defining feature in intrinsic polarity-induced (001) LAO/STO interfacial metallicity. Our results show an inverse relationship between carrier concentration and mobility, thus suggesting that among our samples the higher sheet carrier concentration metallic channels either are thinner spatially or contain more scattering centers. Our hypothesis of localized interfacial holes can be reconciled with both possibilities. However, the dependence of the dielectric constant of STO on carrier concentration and interface electric field cannot be ignored and needs to be examined for a more complete description.

In summary, we have reported an inverse relationship between carrier concentration and mobility, which we speculate to be a defining characteristic of the concomitant generation of carriers and disorder at metallic LAO/STO interfaces induced by polar instability. The transfer of electrons from the LAO side leaves localized holes that can be a source of enhanced interfacial band bending as well as scattering centers for carrier electrons in the metallic channel. In-plane MR measurements reveal larger spin-orbit coupling in higher carrier concentration samples. The interplay between disorder and carrier concentration, and in turn the strength of spin-orbit interaction, is expected to be crucial in the stabilization of different low-temperature interfacial phases at the LAO/STO heterointerface.

The authors thank Michael Flatté for valuable discussions and Kin Man Yu for Rutherford backscattering spectrometry measurements. This research is supported by the Army Research Office under Grant No. MURI W911NF-08-1-0317. The x-ray reflectivity measurements were performed on a facility instrument supported by the Director, Office of Science, Office of Basic Energy Sciences, of the U.S. Department of Energy under Contract No. DE-AC02-05CH11231.

<sup>1</sup>A. Ohtomo and H. Y. Hwang, *Nature (London)* **427**, 423 (2004).

<sup>2</sup>S. Thiel, G. Hammerl, A. Schmehl, C. W. Schneider, and J. Mannhart, *Science* **313**, 1942 (2006).

<sup>3</sup>A. Brinkman, M. Huijben, M. van Zalk, J. Huijben, U. Zeitler, J. C. Maan, W. G. van der Wiel, G. Rijnders, D. H. A. Blank, and H. Hilgenkamp, *Nature Mater.* **6**, 493 (2007).

<sup>4</sup>D. G. Schlom (private communication).

<sup>5</sup>O. Copie *et al.*, *Phys. Rev. Lett.* **102**, 216804 (2009).

<sup>6</sup>N. Reyren *et al.*, *Science* **317**, 1196 (2007).

<sup>7</sup>A. D. Caviglia, S. Gariglio, N. Reyren, D. Jaccard, T. Schneider, M. Gabay, S. Thiel, G. Hammerl, J. Mannhart, and J.-M. Triscone, *Nature (London)* **456**, 624 (2008).

<sup>8</sup>N. Reyren, S. Gariglio, A. D. Caviglia, D. Jaccard, T. Schneider, and J.-M. Triscone, *Appl. Phys. Lett.* **94**, 112506 (2009).

<sup>9</sup>T. Schneider, A. D. Caviglia, S. Gariglio, N. Reyren, and J.-M. Triscone, *Phys. Rev. B* **79**, 184502 (2009).

<sup>10</sup>C. Bell, S. Harashima, Y. Kozuka, M. Kim, B. G. Kim, Y. Hikita, and H. Y. Hwang, *Phys. Rev. Lett.* **103**, 226802 (2009).

<sup>11</sup>M. Ben Shalom, C. W. Tai, Y. Lereah, M. Sachs, E. Levy, D. Rakhmievitch, A. Palevski, and Y. Dagan, *Phys. Rev. B* **80**, 140403(R) (2009).

<sup>12</sup>M. Ben Shalom, M. Sachs, D. Rakhmievitch, A. Palevski, and Y. Dagan, *Phys. Rev. Lett.* **104**, 126802 (2010).

<sup>13</sup>A. D. Caviglia, M. Gabay, S. Gariglio, N. Reyren, C. Cancellieri, and J.-M. Triscone, *Phys. Rev. Lett.* **104**, 126803 (2010).

<sup>14</sup>S. Seri and L. Klein, *Phys. Rev. B* **80**, 180410(R) (2009).

<sup>15</sup>E. Abrahams, P. W. Anderson, D. C. Licciardello, and T. V. Ramakrishnan, *Phys. Rev. Lett.* **42**, 673 (1979).

<sup>16</sup>C. Cen, S. Thiel, G. Hammerl, C. W. Schneider, K. E. Andersen, C. S. Hellburg, J. Mannhart, and J. Levy, *Nature Mater.* **7**, 298 (2008).

<sup>17</sup>C. Bell, S. Harashima, Y. Hikita, and H. Y. Hwang, *Appl. Phys.*

- Lett. **94**, 222111 (2009).
- <sup>18</sup>M. Basletic, J.-L. Maurice, C. Carrétéro, G. Herranz, O. Copie, M. Bibes, E. Jacquet, K. Bouzouane, S. Fusil, and A. Barthélémy, *Nature Mater.* **7**, 621 (2008).
- <sup>19</sup>M. Huijben, G. Rijnders, D. H. A. Blank, S. Bals, S. van Aert, J. Verbeeck, G. van Tendeloo, A. Brinkman, and H. Hilgenkamp, *Nature Mater.* **5**, 556 (2006).
- <sup>20</sup>O. N. Tufte and P. W. Chapman, *Phys. Rev.* **155**, 796 (1967).
- <sup>21</sup>R. Pentcheva and W. E. Pickett, *Phys. Rev. B* **74**, 035112 (2006).
- <sup>22</sup>H. Chen, A. M. Kolpak, and S. Ismail-Beigi, *Phys. Rev. B* **79**, 161402(R) (2009).
- <sup>23</sup>Yu. F. Komnik, V. V. Andrievskii, and I. B. Berkutov, *Low Temp. Phys.* **33**, 79 (2007).
- <sup>24</sup>T. Kawaguti and Y. Fujimori, *J. Phys. Soc. Jpn.* **52**, 722 (1983).
- <sup>25</sup>G. Bergmann, *Phys. Rev. Lett.* **48**, 1046 (1982).
- <sup>26</sup>G. Bergmann, *Solid State Commun.* **42**, 815 (1982).
- <sup>27</sup>P. E. Lindelof and S. Wang, *Phys. Rev. B* **33**, 1478 (1986).
- <sup>28</sup>G. L. Chen, J. Han, T. T. Huang, S. Datta, and D. B. Janes, *Phys. Rev. B* **47**, 4084(R) (1993).